Available online at www.sciencedirect.com

SciVerse ScienceDirect

Ceramics International 38 (2012) 2159–2164

CERAMICS INTERNATIONAL

www.elsevier.com/locate/ceramint

Compaction pressure effect on microstructure and electrochemical performance of $GdBaCo_2O_{5+\delta}$ cathode for IT-SOFCs

Na Li *, Zhe Lü, Bo Wei, Xiqiang Huang, Yaohui Zhang, Wenhui Su

Center for the Condensed Matter Science and Technology, Department of Physics, Harbin Institute of Technology, Harbin 150080, PR China

Received 2 September 2011; received in revised form 20 October 2011; accepted 21 October 2011
Available online 25 October 2011

Abstract

In order to optimize the morphology of starting powder, raw GBCO powder synthesized via solid state reaction was repeatedly compacted by uniaxial die pressing at two apparent compaction pressures of 500 and 1000 MPa. The particle size distribution curves and SEM images indicated that, with increasing compaction pressure and number of compaction times, the larger particles in the powder were gradually broken apart and the particle size became small and uniform. Then the effect of pressing treatment for the starting GBCO particles on the microstructure and performance of sintered cathode was studied. The results demonstrated that, after being sintered under the same conditions, the cathode prepared from the treated GBCO particles showed a finer microstructure compared with that prepared from the raw GBCO particles. In addition, optimizing the morphology of the starting GBCO powder by pressing treatment could improved the cathode performance and made the polarization resistance of final cathode reduce from 1.33 $\Omega\ cm^2$ to 0.40 $\Omega\ cm^2$ at 600 °C.

Keywords: A. Pressing; E. Fuel cells; Cathode; Microstructure

1. Introduction

Recently, much attention has been focused on intermediate-temperature solid oxide fuel cells (IT-SOFCs) operating at ≤800 °C, because the reduced temperature operation can extend the range of material selection, reduce the costs of fabrication and application and improve the stability and reliability for the SOFC systems [1–4]. With the decreasing of operation temperature, however, due to the high activation energy for cathodic reaction, the contribution of the cathode polarization resistance to the total resistance of the cell becomes the dominant contribution in an anode-supported SOFC using membrane electrolyte with low ohmic resistance [5,6]. Hence, great efforts have been paid to reduce the cathode polarization and enhance the electro-catalytic activity of cathode for oxygen reduction reactions (ORRs), so as to improve the performance of IT-SOFC.

Currently, there is considerable number of research activities on the potential of mixed ionic and electronic conductors as cathode materials of IT-SOFCs [7–9]. The mixed conductivity of such materials greatly extends the active oxygen reduction sites from the typical triple phase boundary (TPB) to the entire cathode surface (cathode–gas phase interface), and thereby these materials exhibit high electrochemical activity for oxygen reduction at reduced temperatures [10,11]. Layered Perovskite oxides with general formula of $LnBaCo_2O_{5+\delta}$ (Ln = rare earth, $0 > \delta > 1$) have received tremendous attention as potential alternative MIEC oxides in recent years [12–22]. These compounds exhibit high electronic conductivity and excellent oxygen transport properties (i.e. high oxygen surface exchange coefficient and rapid oxygen–ion diffusion), which are very beneficial for cathodes [19,20,22–24]. According to Kim et al. [19], the oxygen ion diffusivity and surface exchange coefficient of $PrBaCo_2O_{5+\delta}$ were $10^{-5}\ cm^2/s$ and 10^{-3} cm/s at 623 K, respectively, which are higher than typical Perovskite MIECs such as $La_{0.5}Sr_{0.5}CoO_3$, $Sm_{0.5}Sr_{0.5}CoO_3$. In addition, these oxides also demonstrate attractive electrochemical activity. On doped ceria electrolyte and at ~600 °C, the cathodic polarization resistances of $GdBaCo_2O_{5+\delta}$ and $PrBaCo_2O_{5+\delta}$ were reported as 0.58 $\Omega\ cm^2$ and 0.4 $\Omega\ cm^2$, respectively [13,25].

Many studies show that the cathode performance is also heavily dependent on its microstructure in addition to the

* Corresponding author. Tel.: +86 451 86418420; fax: +86 451 86418420.
E-mail addresses: lina19820610@126.com (N. Li), lvzhe@hit.edu.cn (Z. Lü).

0272-8842/$36.00 © 2011 Published by Elsevier Ltd and Techna Group S.r.l.
doi:10.1016/j.ceramint.2011.10.058

intrinsic properties of cathode materials [26–28]. Therefore, the improvement of cathode performance may be realized through optimizing the microstructure of cathode for a given cathode material. The microstructure of the resulting cathode is closely related to the morphological characteristics of the starting powder [29,30], and the morphology of powder could be affected by the synthesis techniques and subsequent treatment processes.

Many different syntheses methods have been developed for production of ceramic powders used as cathode materials in SOFC, such as solid-state reaction, sol–gel technique, co-precipitation, and combustion [31–34]. The solid-state reaction is a conventional method of ceramic processing. Although the sample prepared by solid-state reaction presents larger particle size than the samples prepared by wet chemical methods, the wet chemical methods usually involve complicated process and environmental pollution caused by the emission of noxious gases, e.g. NO_2. Yet solid-state method is capable of circumventing these problems in preparation of ceramic powders. So, in this paper, cathode powder was synthesized by the solid-state reaction method.

The ball-milling and repeated grinding in a mortar are the common methods used to refine the raw powders prepared by solid-state reaction, but these methods are energy-intensive and time-consuming. Therefore, a simple, fast treatment method is needed in order to optimize the morphology of the raw powders.

Forming techniques such as uniaxial compaction pressing, cold isostatic pressing (CIP) have played an important role in production of ceramic materials. These forming processes cannot only press the loose ceramic powder into a mass of certain density and definite shape, but the applied stress during forming also have significant influence on the microstructure and properties of powder. For example, Gao et al. [35] found that the sintering behavior of Y-TZP ceramics compacted by a superhigh pressure can be largely improved because of the increase in contact points between the particles and the decrease in pore size as the applied pressure increased. Lee et al. [36] made Ni–YSZ anode substrate by liquid condensation process under the compaction pressure ranges of 2–7 MPa, and showed that the microstructure (like porosity and pore size) of Ni–YSZ anode substrate can be manipulated by the degree of compaction pressure during forming. In addition, the transition of microstructure with compaction pressure had profound effects on the performance of anode substrate. Kim et al. [37] fabricated the indium tin oxide (ITO) powder compacts by cold isostatic pressing (CIP). Results showed that the inhomogeneity in powder compact was controlled by changing the CIP pressure, and an increase in the forming pressure enhanced the homogeneity of the powder compact.

Uniaxial die pressing is a simple forming technology used to compact the ceramic powders. In the preparation of SOFCs, NiO/YSZ composite powder is usually compacted by this process to form anode substrate [38,39]. In addition, Chen et al. [38,39] found that the applied compaction pressure during forming had great influence on the particle size distributions of raw NiO and YSZ powders. However, up to now, there are few reports about the method of uniaxial pressing used designedly to control the morphology of starting powder as cathode for IT-SOFCs. Therefore, in this paper, the raw GBCO powder prepared by solid-state reaction method was treated by uniaxial die pressing, and then its morphology could be controlled by changing treatment conditions. Moreover, the effect of the morphology of starting powder on microstructure and electrochemical performance of final cathode were investigated.

2. Experimental

$GdBaCo_2O_{5+\delta}$ (GBCO) powder was synthesized by the conventional solid-state reaction method as reported in our previous paper [14]. The raw GBCO powder was repeatedly compacted by uniaxial die pressing at two compaction pressures of 500 and 1000 MPa, respectively. To distinguish these GBCO powders treated under different compaction conditions, they were denoted as various designations, for example, the GBCO powders compacted repeatedly at 1000 MPa pressure for 4 and 6 times were denoted as GBCO1000-4 and GBCO1000-6, respectively. The untreated raw GBCO powder was denoted as GBCO0. The particle size distributions of raw GBCO powder and treated GBCO powders were measured with a laser scattering technique Mastersizer 2000 (Malvern Instruments). The morphology and microstructure of powder and cathode layer were observed by a scanning electron microscope (SEM, Hitachi-S4800).

Symmetrical half cells with the configuration of electrode/electrolyte/electrode were fabricated for electrochemical measurements. In this study, $Sm_{0.2}Ce_{0.8}O_{1.9}$ (SDC) was used as electrolyte material. The SDC powders were uniaxially pressed into pellets under 300 MPa and then sintered at 1400 °C for 4 h in air to obtain dense electrolyte substrates with about 11.5 mm in diameter and 0.5 mm in thickness. In order to improve the adhesion of interface, the surface of SDC pellet was coarsened by spin coating a SDC layer before sintering. Each GBCO powder (raw and treated powders mentioned above) was mixed thoroughly with ethylcellulose–terpineol binder to obtain the corresponding cathode slurry, which was then symmetrically painted on both sides of dense SDC electrolyte pellet to form symmetrical half cell. After drying, these half cells were sintered at 950 °C for 4 h in air. The effective area of cathode was ~0.26 cm^2. Silver paste (DAD-87) was paint onto the electrode surfaces of the symmetrical half cells serving as the current collector and adhereing silver leads.

AC impedance spectroscopy of the symmetrical cells was measured to characterize the electrochemical performance of cathode using impedance response analyzer (Solartron SI 1260) and electrochemical interface (Solartron SI 1287). The impedance data were collected with ZPlot software under open circuit conditions with an AC signal amplitude of 10 mV in a frequency range from 91 kHz to 0.1 Hz, and fitted with ZView 2.3 software. Impedance measurements were taken over a temperature range of 500–700 °C in air.

3. Results and discussion

3.1. Effect of pressing treatment on the morphology of starting powder

The raw GBCO powder prepared by solid-state reaction method usually has a larger grain size and an inhomogeneous size distribution. Fig. 1 shows the particle size distributions of raw and treated GBCO powders. As can be seen, the particle size distribution of the raw GBCO powder (GBCO0) is in a wide range from about 0.67–211 μm, spans three orders of magnitude. This indicates that there are some large aggregates in GBCO0 powder. As shown in Fig. 1, the application of 500 MPa makes the peaks shift to the small size direction and the first peak intensity increase, but which has no obvious effect on the powder size distribution range (see GBCO500-4). This indicates that there are still some larger-size agglomerates in the powder, although some of them have been broken down. However, the powder size distribution becomes considerably narrow when a compaction pressure of 1000 MPa was applied, the upper limit of particle size range is decreased from 211 μm to 21 μm (see GBCO1000-4). This means that particles larger than 21 μm are completely broken down by the additional high stress and then eliminate in GBCO1000-4 powder. Moreover, the first peak is heightened and the second one is lowered, which indicates that particles associated with the second peak are partially crushed into smaller-sized particles.

The SEM micrographs in Fig. 2 show the morphology of GBCO powders compacted repeatedly under a given applied pressure (1000 MPa) with different number of compaction times. Comparing these images, it is evident that GBCO1000-6 powder has smaller and more uniform particle dimensions than GBCO1000-4 and GBCO0 powders have, which indicates that the larger-sized particles in the powder could be gradually broken apart and the morphology of powder gradually becomes finer and more homogeneous with increasing number of compaction times.

From these results, we could know that an increase in either compaction pressure or number of compaction times during treatment process might effectively enhance the homogeneity of the raw powder by crushing large particles, and make powder have small and uniform particle dimensions. Therefore, uniaxial compaction pressing could be used as a simple and effective processing method of optimizing the morphology of raw powder by changing the processing parameters (such as compaction pressure and the number of compaction times).

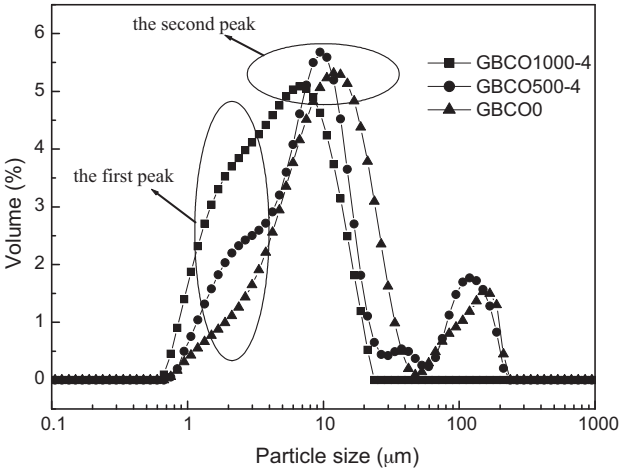

Fig. 1. Particle size distributions of the starting GBCO powders treated under different conditions.

3.2. Effect of the starting powder treated by pressing on the cathode microstructure and performance

Fig. 3a shows the electrochemical impedance spectra of the symmetrical half cells with different cathodes at 600 °C in air. An equivalent circuit is given in Fig. 3b for data analysis. In the circuit, L is the cable inductance arising from the measurement apparatus. R_0 is attributed to the overall ohmic resistance including the electrolyte resistance, the electrode ohmic resistance, the lead resistance and the contact resistance between electrode and electrolyte. (R_1–CPE_1) and (R_2–CPE_2) represent the high frequency arc and low frequency arc, respectively, where R is the resistance of the corresponding arc, and CPE is the corresponding constant phase element for each arc. The impedance spectra are fitted well by this model $LR_0(R_1CPE_1)(R_2CPE_2)$, and the fitting results indicate that there are at least two electrode processes corresponding to the high and low frequency arcs during the overall oxygen reduction reaction (ORR). The high frequency arc could be attributed to the charge transfer process. The low frequency arc

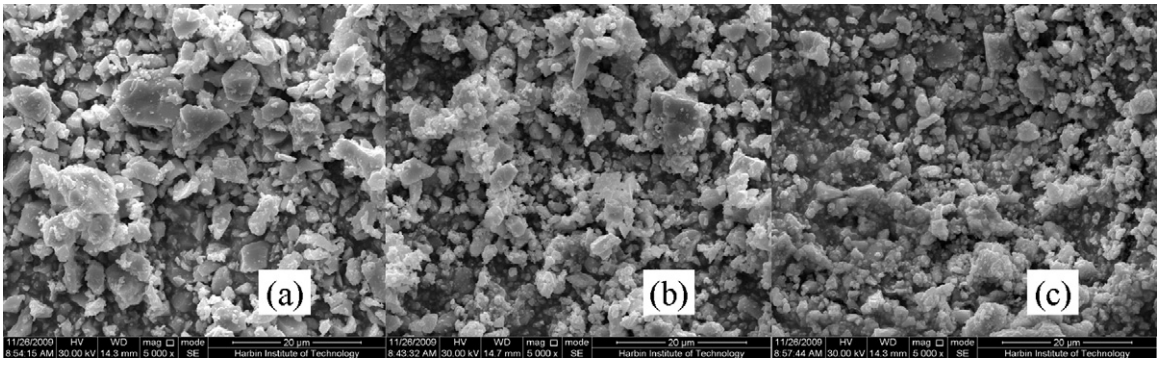

Fig. 2. Typical SEM micrographs of (a) GBCO1000-1, (b) GBCO1000-4, and (c) GBCO1000-6 powders.

Table 1
Typical fitting parameters for impedance spectra of various GBCO cathodes at 600 °C.

Sample	R (Ω cm^2)			
	R_0	R_1	R_2	$R_p = R_1 + R_2$
GBCO0	1.19	0.56	0.77	1.33
GBCO500-4	1.17	0.30	0.57	0.87
GBCO1000-4	1.08	0.16	0.35	0.51
GBCO1000-6	1.03	0.10	0.30	0.40

could be attributed to the oxygen adsorption and desorption on the cathode surface and surface oxygen diffusion process [40–42]. The sum of R_1 and R_2 corresponds to the total polarization resistance R_p of cathode, which is corrected for electrode area and divided by two in order to obtain area-specific polarization resistance (in Ω cm^2). Cathode polarization resistance (R_p) is a significant index used to evaluate the performance of cathode. Typical fitting parameters R_0, R_1, R_2, and R_p (derived from Fig. 3a) are listed in Table 1. It is clear that cathodes prepared from treated GBCO powders exhibit lower R_0, R_1, and R_2 compared with that prepared from raw GBCO powder when all ones are sintered under the same conditions (i.e. 950 °C for 4 h). Moreover, based on the previous analysis to the morphology of the starting GBCO powders, it can be found that the cathode made from smaller and more uniform GBCO particles exhibits lower resistance and better electrochemical performance. So pressing treatment for starting powder is helpful to improving cathode performance. The lowest R_p of GBCO cathodes in this study (i.e. 0.40 Ω cm^2 at 600 °C) is smaller than the literature results. For example, the R_p values of GBCO cathodes were reported as 0.58 Ω cm^2 [25] or 1.35 Ω cm^2 [21] at ∼600 °C. In addition, as shown in Table 1, R_2 values are larger than R_1 ones for all the measured cathodes. This phenomenon suggests that optimizing in the morphology of starting GBCO powder in this study does not change the cathode reaction processes, but accelerates the reaction rates.

The variations in R_p (i.e. R_1 and R_2) for GBCO cathodes might be associated with the micro-structural change induced by various starting GBCO powder, because all other conditions (include sintering temperature and time) are same. In addition, it is well known that oxygen reduction process strongly depends on the microstructure of the cathode, in particular, the particle

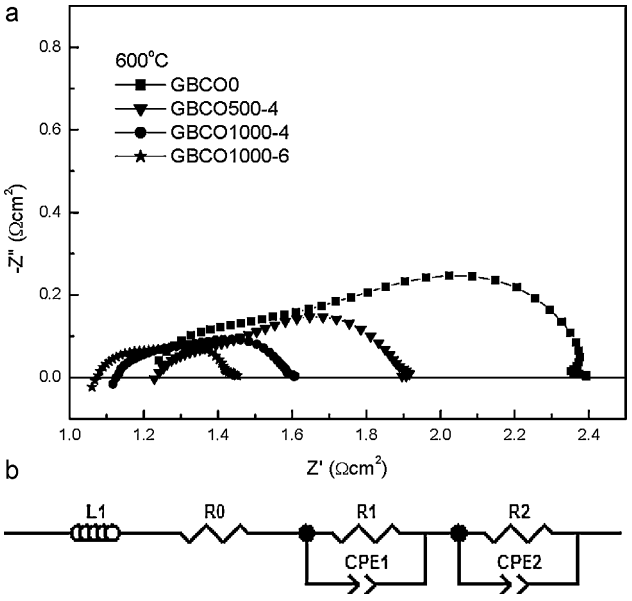

Fig. 3. (a) Impedance spectra measured at 600 °C in air for various GBCO cathodes sintered at 950 °C for 4 h. (b) The equivalent circuit for data fitting.

size of the cathode material [11]. Fig. 4 shows the cross-sectional SEM images of GBCO0, GBCO500-4 and GBCO1000-4 cathodes sintered at 950 °C for 4 h. It can be readily observed that the microstructures of cathodes prepared from various GBCO powders are very different. The GBCO1000-4 cathode has a smaller particle size and a more homogeneous particle size distribution than GBCO500-4 and GBCO0 cathode. This phenomenon confirms that the morphology of the starting powder has a great influence on the final cathodic microstructure. The decrease of R_1 and R_2 can be explained by the following reasons. On the one hand, the smaller and more homogeneous particles could create more particle-to-particle contact points and subsequently lead to an increase in number of electron and oxygen ion conduction paths, which accelerate the charge transportation from particle to particle in the electrode. On the other hand, the use of small particles could increase the electrode surface area (gas–solid phase interface) for oxygen adsorption, dissociation, and surface diffusion, therefore promote the oxygen adsorption/desorption and surface oxygen diffusion processes, resulting in

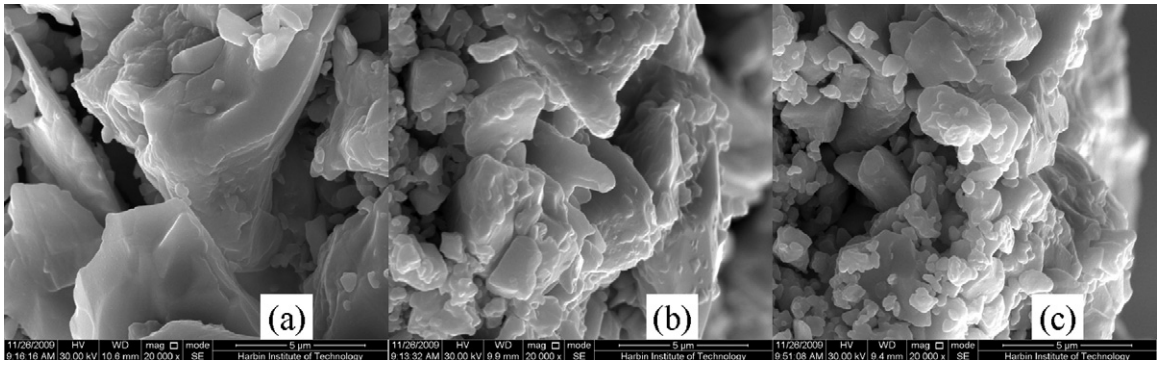

Fig. 4. SEM cross-sectional views of various cathodes made from (a) GBCO0, (b) GBCO500-4, and (c) GBCO1000-4 powders, sintered at 950 °C for 4 h.

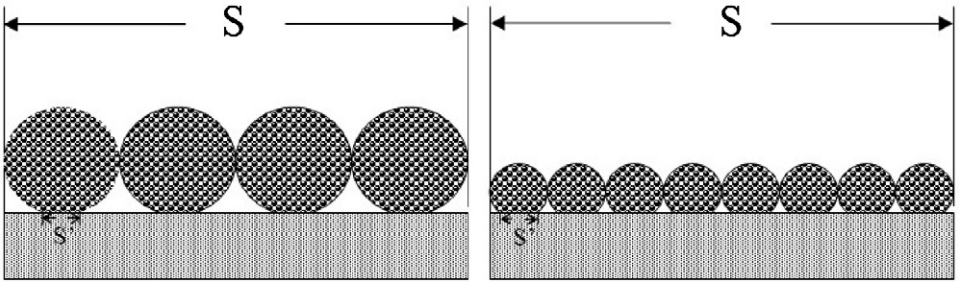

Fig. 5. Schematic diagrams of the interface between electrode and electrolyte.

the decrease of R_2 (corresponding to the resistance of this process). In addition, the charge transfer process of oxygen reduction reaction also occur on the cathode surface, thereby the smaller grain size with high specific surface area also bring the reduction of R_1 (corresponding to the resistance of charge transfer process).

The variation of R_0 could be contributed to the microstructural change of the interface between electrode and electrolyte. Due to the porosity of the electrode, the contact regions between cathode and electrolyte are not continuous but consist of many discrete contact points, while the imperfect interface contact make contact resistance play an important role in the ohmic losses. Schematic diagrams of the interface model are shown in Fig. 5. The geometry of the contact point is defined as round in contact model. At the same sintering conditions, the area of every contact point (S') may be considered to be the same. In addition, the total area of electrode/electrolyte interface (S) is also identical (~0.26 cm^2). In the case, contact resistance strongly depends on the number of contact points at electrode/electrolyte interface, while this number could be controlled mainly by the particle size of cathode. It is considered that the use of the smaller GBCO particles allows more contact points, and lead to the reduction in contact resistance. Based on the above mentioned research, the particle size distribution became considerably narrow, and particles larger than 21 μm were completely eliminated when a compaction pressure of 1000 MPa was applied (see Fig. 1), therefore the GBCO1000 cathode comprised of the smaller size particles exhibits an reduction in ohmic resistance compared with GBCO500-4 and GBCO0 cathodes (see Table 1).

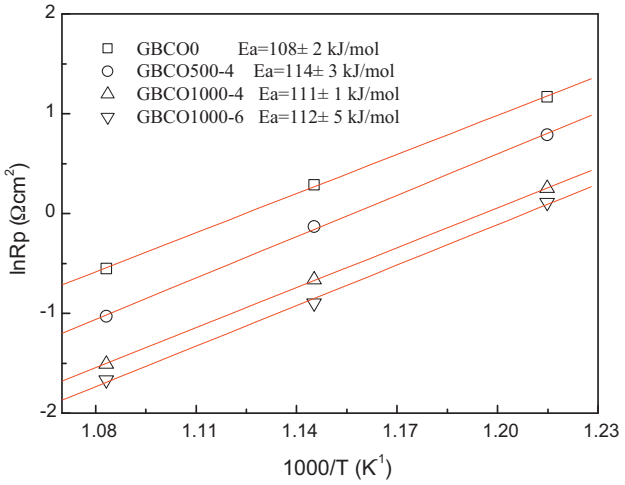

Fig. 6. Arrhenius plots of the R_p values for different GBCO cathodes.

Fig. 6 shows Arrhenius plots of the R_p values for various GBCO cathodes. The activation energy can be calculated from the slope of the fitted line. The activation energies for all cathodes are around 111 kJ/mol, and these values are similar to those reported in the literature [40,41]. In addition, the values of their activation energies are very close indicating the same mechanism of the electrode reactions. This result well agrees with the resistance results above.

4. Conclusions

Uniaxial die pressing treatment could be used as a simple and effective method of optimizing the morphology of raw powder. With the increase of applied pressure and number of pressing times, the larger particles in powder were gradually broken down and particles became small and homogeneous. Under the same sintering conditions, cathodic microstructure was strongly influenced by the morphology of starting powder. The cathode prepared from the treated GBCO particles had finer microstructure than that prepared from the raw particles. EIS tests revealed that the cathode prepared from the treated GBCO particles had lower ohmic resistance and polarization resistance than that prepared from the untreated GBCO particles. The variation of R_o and R_p values for various GBCO cathodes could be attributed to the microstructural changes of the interface (between cathode and electrolyte) and cathode induced by the starting powders with different particle sizes (resulted by pressing treatment), respectively.

Acknowledgements

This work was supported by Ministry of Science and Technology of China (2007AA05Z139) and the Natural Science Foundation of China (20901020). This work was also supported by Natural Scientific Research Innovation Foundation in Harbin Institute of Technology (HIT. NSRIF. 2009057).

References

[1] A.J. Jacobson, Materials for solid oxide fuel cells, Chem. Mater. 22 (2010) 660–674.
[2] Z.P. Shao, S.M. Haile, A high-performance cathode for the next generation of solid–oxide fuel cells, Nature 431 (2004) 170–173.
[3] S.C. Singhal, Solid oxide fuel cells for stationary mobile, and military applications, Solid State Ionics 152-153 (2002) 405–410.

[4] M. Dokiya, SOFC system and technology, Solid State Ionics 152-153 (2002) 383–392.
[5] S.B. Adler, Factors governing oxygen reduction in solid oxide fuel cell cathodes, Chem. Rev. 104 (2004) 4791–4843.
[6] C.R. Xia, W. Rauch, F.L. Chen, M.L. Liu, $Sm_{0.5}Sr_{0.5}CoO_3$ cathodes for low-temperature SOFCs, Solid State Ionics 149 (2002) 11–19.
[7] S.J. Skinner, Recent advances in Perovskite-type materials for solid oxide fuel cell cathodes, Int. J. Inorg. Mater. 3 (2001) 113–121.
[8] J. Sacanell, M.G. Bellino, D.G. Lamas, A.G. Leyva, Synthesis and characterization $La_{0.6}Sr_{0.4}CoO_3$ and $La_{0.6}Sr_{0.4}Co_{0.2}Fe_{0.8}O_3$ nanotubes for cathode of solid–oxide fuel cells, Physica B 398 (2007) 341–343.
[9] J.W. Yun, S.P. Yoon, S. Park, J. Han, S.W. Nam, T.H. Lim, et al., Modifying the cathodes of intermediate-temperature solid oxide fuel cells with a $Ce_{0.8}Sm_{0.2}O_2$ sol–gel coating, Int. J. Hydrogen Energy 34 (22) (2009) 9213–9219.
[10] M. Koyama, C.J. Wen, T. Masuyama, J. Otomo, H. Fukunaga, K. Yamada, et al, The mechanism of porous $Sm_{0.5}Sr_{0.5}CoO_3$ cathodes used in solid oxide fuel cells, J. Electrochem. Soc. 148 (7) (2001) A795–A801.
[11] S.B. Adler, Mechanism and kinetics of oxygen reduction on porous $La_{1-x}Sr_xCoO_{3-\delta}$ electrodes, Solid State Ionics 111 (1998) 125–134.
[12] H.T. Gu, H. Chen, L. Gao, Y.F. Zheng, X.F. Zhu, L.C. Guo, Oxygen reduction mechanism of $NdBaCo_2O_{5+\delta}$ cathode for intermediate-temperature solid oxide fuel cells under cathodic polarization, Int. J. Hydrogen Energy 34 (2009) 2416–2420.
[13] D.J. Chen, R. Ran, K. Zhang, J. Wang, Z.P. Shao, Intermediate-temperature electrochemical performance of a polycrystalline $PrBaCo_2O_{5+\delta}$ cathode on samarium-doped ceria electrolyte, J. Power Sources 188 (2009) 96–105.
[14] N. Li, Z. Lü, B. Wei, X.Q. Huang, K.F. Chen, Y.H. Zhang, et al, Characterization of $GdBaCo_2O_{5+\delta}$ cathode for IT-SOFCs, J. Alloy Compd. 454 (2008) 274–279.
[15] K. Zhang, L. Ge, R. Ran, Z.P. Shao, S.M. Liu, Synthesis, characterization and evaluation of cation-ordered $LnBaCo_2O_{5+\delta}$ as materials of oxygen permeation membranes and cathodes of SOFCs, Acta Mater. 56 (2008) 4876–4889.
[16] J.H. Kim, A. Manthiram, $LnBaCo_2O_{5+\delta}$ oxides as cathodes for intermediate-temperature solid oxide fuel cells, J. Electrochem. Soc. 155 (2008) B385–B390.
[17] Q.J. Zhou, T.M. He, Y. Ji, $SmBaCo_2O_{5+x}$ double-Perovskite structure cathode material for intermediate-temperature solid oxide fuel cells, J. Power Sources 185 (2008) 754–758.
[18] B. Lin, S.Q. Zhang, L.C. Zhang, L. Bi, H.P. Ding, X.Q. Liu, et al., Protonic ceramic membrane fuel cells with layered $GdBaCo_2O_{5+x}$ cathode prepared by gel-casting and suspension spray, J. Power Sources 177 (2008) 330–333.
[19] G. Kim, S. Wang, A.J. Jacobson, L. Reimus, P. Brodersen, C.A. Mims, Rapid oxygen ion diffusion and surface exchange kinetics in $PrBaCo_2O_{5+x}$ with a Perovskite related structure and ordered A cations, J. Mater. Chem. 17 (2007) 2500–2505.
[20] A. Tarancon, S.J. Skinner, R.J. Chater, F. Hernandez-Ramirez, J.A. Kilner, Layered Perovskites as promising cathodes for intermediate temperature solid oxide fuel cells, J. Mater. Chem. 17 (2007) 3175–3181.
[21] A.M. Chang, S.J. Skinner, J.A. Kilner, Electrical properties of $GdBaCo_2O_{5+x}$ for IT-SOFC applications, Solid State Ionics 177 (2006) 2009–2011.
[22] A.A. Taskin, A.N. Lavrov, Y. Ando, Achieving fast oxygen diffusion in Perovskites by cation ordering, Appl. Phys. Lett. 86 (2005) 091910.
[23] T. Vogt, P.M. Woodward, P. Karen, B.A. Hunter, P. Henning, A.R. Moodenbaugh, Low to high spin-state transition induced by charge ordering in antiferromagnetic $YBaCo_2O_5$, Phys. Rev. Lett. 84 (2000) 2969–2972.
[24] A. Maignan, C. Martin, D. Pelloquin, N. Nguyen, B. Raveau, Structural and magnetic studies of ordered oxygen-deficient Perovskites $LnBaCo_2O_{5+\delta}$, closely related to the 112 structure, J. Solid State Chem. 142 (1999) 247–260.
[25] A. Tarancon, J. Pena-Martinez, D. Marrero-Lopez, A. Morata, J.C. Ruiz-Morales, P. Nunez, Stability, chemical compatibility and electrochemical performance of $GdBaCo_2O_{5+x}$ layered Perovskite as a cathode for intermediate temperature solid oxide fuel cells, Solid State Ionics 179 (2008) 2372–2378.
[26] Y.J. Leng, S.H. Chan, Q.L. Liu, Development of LSCF-GDC composite cathodes for low-temperature solid oxide fuel cells with thin film GDC electrolyte, Int. J. Hydrogen Energy 33 (2008) 3808–3817.
[27] F. Tietz, A. Mai, D. Stöver, From powder properties to fuel cell performance-A holistic approach for SOFC cathode development, Solid State Ionics 179 (2008) 1509–1515.
[28] M.J. Jorgensen, S. Primdahl, C. Bagger, M. Mogensen, Effect of sintering temperature on microstructure and performance of LSM–YSZ composite cathodes, Solid State Ionics 139 (2001) 1–11.
[29] K. Murata, T. Fukui, H. Abe, M. Naito, K. Nogi, Morphology control of $La(Sr)Fe(Co)O_{3-a}$ cathodes for IT-SOFCs, J. Power Sources 145 (2005) 257–261.
[30] H.S. Song, W.H. Kim, S.H. Hyun, J. Moon, J. Kim, H.W. Lee, Effect of starting particulate materials on microstructure and cathodic performance of nanoporous LSM–YSZ composite cathodes, J. Power Sources 167 (2007) 258–264.
[31] C.J. Fu, K.N. Sun, X.B. Chen, N.Q. Zhang, D.R. Zhou, Electrochemical properties of A-site deficient SOFC cathodes under Cr poisoning conditions, Electrochim. Acta 54 (2009) 7305–7312.
[32] R. Chiba, F. Yoshimura, Y. Sakurai, Y. Tabata, M. Arakawa, A study of cathode materials for intermediate temperature SOFCs prepared by the sol–gel method, Solid State Ionics 175 (2004) 23–27.
[33] A. Tarancón, D. Marrero-López, J. Peña-Martínez, J.C. Ruiz-Morales, P. Núñez, Effect of phase transition on high-temperature electrical properties of $GdBaCo_2O_{5+x}$ layered Perovskite, Solid State Ionics 179 (2008) 611–618.
[34] M. Bevilacqua, T. Montini, C. Tavagnacco, G. Vicario, P. Fornasiero, M. Graziani, Influence of synthesis route on morphology and electrical properties of $LaNi_{0.6}Fe_{0.4}O_3$, Solid State Ionics 177 (2006) 2957–2965.
[35] L. Gao, W. Li, H.Z. Wang, J.X. Zhou, Z.J. Chao, Q.Z. Zai, Fabrication of nano Y-TZP materials by superhigh pressure compaction, J. Eur. Ceram. Soc. 21 (2001) 135–138.
[36] D.S. Lee, J.H. Lee, J. Kim, H.W. Lee, H.S. Song, Tuning of the microstructure and electrical properties of SOFC anode via compaction pressure control during forming, Solid State Ionics 166 (2004) 13–17.
[37] B.C. Kim, J.H. Lee, J.J. Kim, Effect of forming pressure on densification behavior of nanocrystalline ITO powder, J. Eur. Ceram. Soc. 27 (2007) 807–812.
[38] K.F. Chen, X.J. Chen, Z. Lü, N. Ai, X.Q. Huang, W.H. Su, Performance evolution of NiO/yttria-stabilized zirconia anodes fabricated at different compaction pressures, Electrochim. Acta 54 (2009) 1355–1361.
[39] K.F. Chen, Z. Lü, N. Ai, X.J. Chen, X.Q. Huang, W.H. Su, Experimental study on effect of compaction pressure on performance of SOFC anodes, J. Power Sources 180 (2008) 301–308.
[40] B. Wei, Z. Lü, T.S. Wei, D.C. Jia, X.Q. Huang, Y.H. Zhang, J.P. Miao, W.H. Su, Nanosized $Ce_{0.8}Sm_{0.2}O_{1.9}$ infiltrated $GdBaCo_2O_{5+\delta}$ cathodes for intermediate-temperature solid oxide fuel cells, Int. J. Hydrogen Energy 36 (2011) 6151–6159.
[41] B. Wei, Z. Lü, D.C. Jia, X.Q. Huang, Y.H. Zhang, W.H. Su, Thermal expansion and electrochemical properties of Ni-doped $GdBaCo_2O_{5+\delta}$ double-Perovskite type oxides, Int. J. Hydrogen Energy 35 (2010) 3775–3782.
[42] F.H. van Heuveln, H.J.M. Bouwmeester, Electrode properties of Sr-doped $LaMnO_3$ on yttria-stabilized zirconia. 2. Electrode kinetics, J. Electrochem. Soc. 144 (1997) 134–140.